Agricultural Science; Vol. 4, No. 2; 2022
ISSN 2690-5396 E-ISSN 2690-4799
https://doi.org/10.30560/as.v4n2p66

# Design And Experiment of Axial Air-Suction Drum Seed-Metering Device

Yuqian Zhang[1], Chengyao Zhang[1], Yuwei Hu[1], Long Chen[1], Wencai Yang[1] & Haidong Zhang[1]

[1] Faculty of Mechanical and Electrical Engineering, Yunnan Agricultural University, Kunming, Yunnan, P. R. China

Correspondence: Haidong Zhang, Faculty of Mechanical and Electrical Engineering, Yunnan Agricultural University, Kunming, Yunnan, P. R. China. E-mail: zhd74@126.com

Received: November 30, 2022 Accepted: December 15, 2022 Online Published: December 16, 2022

*The research is financed by (Major science and technology projects in Yunnan Province (grant number 202102AE090042-06) and Major science and technology projects in Yunnan Province (grant number 2018ZC001-4).*

**Abstract**

This study developed an axial air-suction drum seed-metering device without a special vacuum pump and associated pipeline facilities, greatly simplifying the structure of the air-suction drum seed-metering device, which aimed to solve the problems of complex structure and difficult maintenance of traditional air suction drum seed-metering device. The geometric model of the seed-metering device was established by SOLIDWORKS. In addition, numerical simulation tests were carried out on the seed-metering device based on CFD to verify the feasibility of the theoretical operation of the seed-metering device. The seed-metering device was processed and a test bench was built for physical testing, which verified the feasibility of the actual operation of the seed-metering device. The bench test results showed that when the fan speed reached 2100 rpm, the adsorption rate of the seed-metering device on tomato seeds, pepper seeds, and eggplant seeds reached more than 86.39%,87.22%, and 93.06%, respectively. Besides, when the fan speed reached 2400 rpm, the adsorption rate of the seed-metering device on tomato seeds, hot pepper seeds, and eggplant seeds all reached more than 95%, which demonstrated that the seed-metering device has good seed suction performance despite its straightforward design.

**Keywords:** axial air-suction, drum, seed-metering device, Computational Fluid Dynamics(CFD), numerica l simulation, experiment

## 1. Introduction

China is the world's greatest producer and consumer of vegetables, and in recent years, the proportion of vegetables in crops has surpassed that of grains to take the top spot. (Wang, L. H., 2016) Cabbage, tomato, hot pepper, eggplant, etc. are all vegetable crops. At present, there are a variety of planting methods for vegetable crops in China, among which manual sowing and precision planter seeding in facilities account for the vast majority. Traditional hand sowing is labor-intensive in the field and inefficient. (Li, Z. G., 2022) Also, it seriously wastes seeds, leading to an increase in production costs and the inability to ensure the sowing quality. On the contrary, the use of precision seeders equipped with facilities can improve land utilization, alleviate seasonal conflicts, improve seedling conditions, and increase yield and income. (Yang, C. M., 2022) However, the vegetable precision seeder suitable for facility seedling cultivation in China has few models and poor seeding effect, which can not meet the operation requirements well. Therefore, it is of great significance to develop vegetable sowing equipment with high efficiency and quality for improving the level of vegetable sowing mechanization in China, reducing labor costs, saving seeds, promoting vegetable farmers' income, increasing production, and ensuring sustainable development of China's vegetable industry. (Zhao, R., 2022)

The seed-metering device is the core component that determines the sowing performance of the precision seeder. It has a direct impact on the seeder's energy consumption, sowing efficiency, uniformity, seed damage rate, and other performance indicators, which in turn has a direct impact on crop production, quality, and cost. (Zhu LT, 2022) According to its working principle, the seed-metering device can be divided into the mechanical type and pneumatic type. Currently, mechanical seed-metering equipment is still widely used in China, largely due to its straightforward construction and affordable manufacturing and maintenance. (Zhang, X. L., 2020). However, the

mechanical seed-metering device has strict requirements on the shape and quality of the seeds. Vegetable seeds should be pelleted before being sown using a mechanical seed-metering system. otherwise, the seeds will be harmed and the efficiency of vegetable production will be compromised. With the continuous development of large-scale production, vegetable farmers have put forward higher requirements for the sowing quality and sowing speed of vegetable seeders, prompting vegetable seeder developers to further explore a new type of pneumatic sowing form. Pneumatic seeder has small damage to seeds, good versatility, low requirements for seed size and quality, high sowing precision, good quality, high efficiency, reliable work, and is suitable for high-speed operation. (D. Karayel,2009). Therefore, it has gradually become the research object of many experts and scholars in recent years. Ding et al. (Ding L, 2018) designed a high-speed precision seed-metering device with air suction for corn with the function of assisting seed filling, which disturbed the seeds in the seed filling area by using the shaped hole boss, and could achieve uniform seed-metering in the seed unloading area, greatly improving the qualification index. Zhang et al. (Zhang, X. H., 2018) studied the mechanism of pneumatic centralized wheat seed-metering and distribution and designed a pneumatic centralized wheat seed-metering and distribution system, which effectively solved the problem of uneven sowing during wheat sowing, and provided a reference for wide sowing. The precision seed-metering device designed by Yin et al. (Yin, W. Q., 2019) used a two-stage seed-metering method. The first stage used a small structure grooved wheel seed-metering device for seed-metering, and the second stage used a pneumatic seed-metering device with negative pressure suction and positive pressure injection for seed-metering. The 3D dimensions of pakchoi, radishes, and eggplants were measured by 3D laser scanning and 3D point cloud computing methods, and based on this, a variety of nozzle types such as straight holes, tapered holes, and cylindrical holes were designed. Through the single-factor experiment, it was concluded that the suitable sucking nozzle holes for seed arrangement of pakchoi, radish and eggplant were cone holes, round waist holes, and straight holes, respectively. Yang et al. (Yang CM,2020)designed a kind of pneumatic cylinder precision seeder similar to a small precision seeding assembly line by using the vacuum adsorption principle, which could complete the whole process from the seedling tray to the foundation covering. The pneumatic cylinder was used to realize continuous seeding, which improved the seeding efficiency. The stepping motor and synchronous belt drive were used to ensure the seeding accuracy. Xu et al. (Xu SY,2020) designed a pneumatic disc-type precision metering device for carrots, which absorbed seeds by negative pressure, and used a seed filling device, a seed cleaning device, the gravity and collision principle, and a blockage removal device to carry out the process of auxiliary seed filling, seed cleaning, seed dropping and positive pressure blockage removal in turn. Ji et al. (Ji, Y., 2021) designed an air-suction double-layer drum precision metering device, which adopts the combination of the double-layer drum and independent air passage technology to reduce the pneumatic parameter requirements of rice seeds on the metering device. Zhang et al. (Zhang. H., 2019) put forward a new idea of printing a split-type negative pressure seed suction drum with 3D rapid prototyping technology, and innovatively designed a double chamber seed-metering drum. With tomato seeds as the experimental object, the orthogonal regression experiment was carried out with the rotating speed of the drum, the negative pressure of the drum and the positive pressure of the air chamber in the seed feeding chamber as the experimental factors, and the variance analysis and regression fitting of the experimental data were carried out using Design Expert. The significance of the negative pressure of the drum, the rotating speed of the drum, and the positive pressure of the air chamber in the seed feeding chamber that affected the seed-metering performance indexes was analyzed, and the better structural parameters and working parameters that affected the seed-metering performance indexes were determined. Chen et al. (Chen, H. T., 2020) designed a three-leaf type automatic seed cleaning and changing air suction seed-metering device for soybean breeding, used EDEM virtual simulation to analyze the auxiliary seed filling process, and determined the leaf inclination angle when achieving the best auxiliary seed filling effect. According to the agronomic requirements of plot breeding, with the operation speed, vacuum degree, seed clearing and changing time as the experimental factors, and the qualification index, replanting index, missed seeding index, and seed clearing and changing distance as the experimental indicators, the three-factor five-level quadratic orthogonal rotation center combination experiment was conducted, and the best working parameter combination of the seed-metering device was obtained.

In summary, although experts and scholars have made a lot of research and improvement on the structure of the seed-metering device, which has improved the seeding efficiency and the seeding qualification index of the precision seeder, there are still some shortcomings such as the complex structure and difficult maintenance. (Liu, Y., 2022) In particular, the air suction drum seed-metering device used in some vegetable plug seedling production lines needs to be equipped with a pressure zone and a negative pressure zone in the cylindrical drum (Sun, H., 2021) and fix multiple pipes (holes). The processing, assembly, and maintenance are very complicated and the cost is very high. Therefore, it is necessary to carry out innovative design and research on the air suction seed-metering device and explore new air suction methods and principles to overcome the defects of the existing air suction seed-metering device.

## 2. Structure and Working Principle of the Seed-Metering Device

Figure 1 depicts the general construction of the new type (axial flow) air suction drum seed-metering device developed in this article. Its components included the drum retaining ring, drum, seed box, transmission shaft, fan blade, fan leaf retaining ring, etc. The drum retainer ring was connected to the drum through screws, and its main function was to connect the induction reducer motor to drive the seed-metering drum to rotate. To support the transmission shaft, which was rotated by the Puss reducer motor, a bearing was put in place at the center of the drum retainer ring and the fan retainer ring. The bottom of the seed box served as a seed scraper.

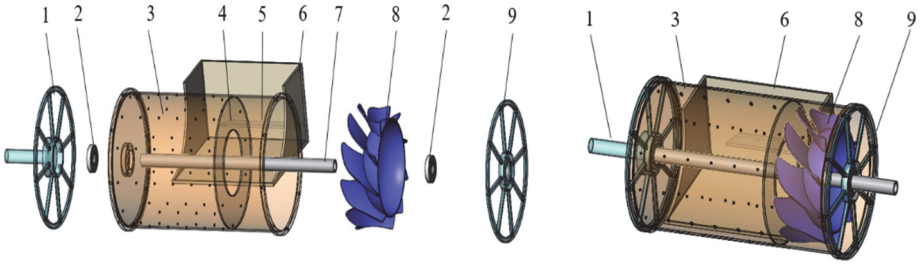


a b

Figure 1. Structure diagram of seed-metering device: (a) exploded view. (b) assembly diagram. 1. Drum retaining ring 2. Bearing; 3. Drum 4. Annular partition 5. Fan blade air chamber 6. Seed box 7. Transmission shaft 8. Fan blade 9. Fan blade retainer

The working process of the seed-metering device was mainly divided into three stages: seed suction I, seed carrying II, and seed feeding III, of which the seed suction stage was the most critical, and was also the focus of this paper. The first thing that happened during the operation was for the fan to rotate to exhaust the gas from the fan air chamber's right side. To absorb the seeds at this point, negative pressure was created at the molded hole. The seeds then rotated together as the drum carries them. The seed-metering procedure was finished when the seed flowed along the drum to its lowest point and was scraped off by the seed scraper at the base of the seed box. The working process as shown in Figure 2.

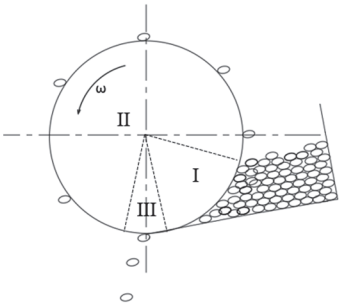


Figure 2. Operating principle of seed metering device: I Seed sucking area; II. Seed carrying area; Ⅲ. Seed feeding area

## 3. Parameter Design of Key Components of the Seed-Metering Device

The seed suction performance of the axial air-suction drum seed-metering device is closely related to the structural parameters, such as the shape and size of the shaped hole, the diameter of the drum, the structural distribution, etc. To ensure the seed suction efficiency of the seed metering device, the structure and parameters of the above key components should be determined.

### *3.1 Design of Shaped Hole*

The holes on the circumference of the drum directly determine the effect of seed adsorption. The diameter of the shaped hole entrance is closely related to the three-dimensional size of the seed. Therefore, this paper took tomato,

hot pepper, and eggplant seeds as the research object, and measured the three-dimensional size of three kinds of seeds. Test seeds were obtained from legal online sources. Table 1 shows the average triaxial size measured in the experiment, and Figure 3 shows the seed size distribution.

Table 1. Seed triaxial size

| Parameter | Seed Type | | |
|---|---|---|---|
| | Tomato | Hot pepper | Eggplant |
| Average length /mm | 3.46 | 3.72 | 3.11 |
| Average width /mm | 2.38 | 3.04 | 2.58 |
| Average thickness /mm | 0.66 | 0.76 | 0.79 |

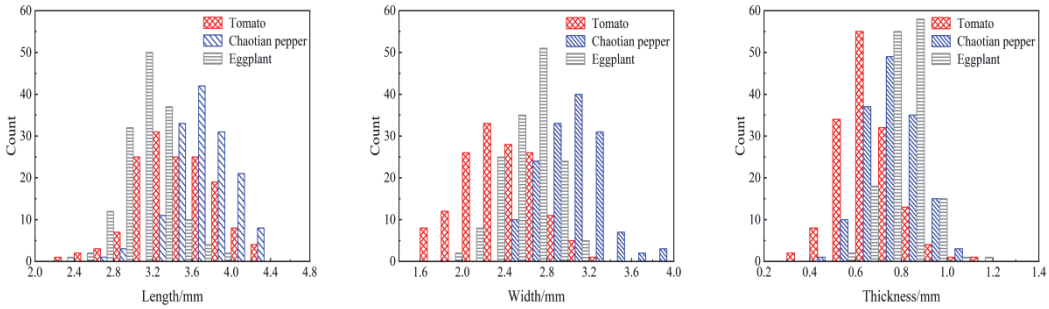


a b c

Figure 3. Triaxial size distribution of seeds: (a) length distribution (b) width distribution (c) thickness distribution

Table 1 shows that the three kinds of seeds had large differences in three-dimensional dimensions, and the thickness was far less than the length and width. They are flat seeds, so the size of the hole entrance should be designed according to the width of the seeds. Figure 4 shows that the three seed sizes all obeyed the approximately normal distribution, indicating that the seed size data were true and reliable. To ensure that no seed was sucked into the hole inlet, the tomato seed with the smallest width must be used as a reference, according to Formula (1)(Jiang YZ,2019)

$$d = 0.64 \sim 0.66b \tag{1}$$

It can be obtained that the inlet diameter of the molded hole d ≈ 1.52~1.57mm, taking d=1.57mm.

According to the law of conservation of mass, the mass of the fluid system in any flow field remains unchanged in the process of moving. Assuming that the fluid is homogeneous and incompressible, the flow continuity equation can be obtained, as shown in Formula (2).

$$V_1 A_1 = V_2 A_2 \tag{2}$$

Where $V_1$ is the speed of section 1 (m/s), $V_2$ is the speed of section 2 (m/s), $A_1$ is the area of section 1 ($m^2$), and $A_2$ is the area of section 1 ($m^2$).

According to Newton's law of mechanics, assuming that the fluid flows under incompressible, inviscid, non-volume force (without considering gravity) and constant flow, the Bernoulli equation of the flow process is：

$$\frac{P_1}{\rho g} + \frac{V_1^2}{2g} + Z_1 = \frac{P_2}{\rho g} + \frac{V_2^2}{2g} + Z_2 \tag{3}$$

Where $P_1$ is the pressure of section 1 (Pa), $P_2$ is the pressure of section 2 (Pa), $Z_1$ is the height of section 1 (millimeter), $Z_2$ is the height of section 1 (millimeter), and $\rho$ is the fluid density (Kg/m ³), $g$ is the acceleration of gravity ($m/s^2$).

Since the length of the molded hole is only 2.5mm, it can be approximately considered that the height of the molded hole inlet and the bottom of the molded hole are equal, that is, $Z_1$=$Z_2$, then the formula can be obtained:

$$\begin{cases} V_1 A_1 = V_2 A_2 \\ \dfrac{P_1}{\rho g} + \dfrac{V_1^2}{2g} = \dfrac{P_2}{\rho g} + \dfrac{V_2^2}{2g} \end{cases} \tag{4}$$

It can be seen from Formula 3 that the velocity increases with the decrease of the section, and the pressure decreases at this time. In other words, the negative pressure will increase with the increase of the flow rate. Therefore, to obtain a better negative pressure effect at the molded hole, a molded hole with a variable section shape should be designed, and the diameter of the molded hole inlet should be smaller than the diameter of the bottom outlet of the molded hole. The molded hole structure is shown in Figure 4.

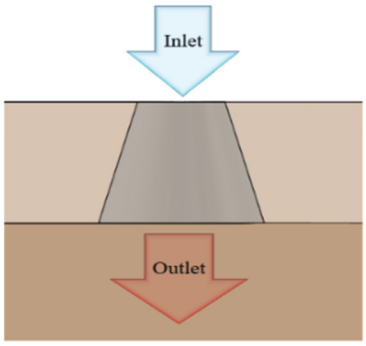


Figure 4. Schematic Diagram of Shaped Hole Structure

*3.2 Drum Design*

The seed metering drum is crucial for ensuring that the seed is sown precisely by the seed metering mechanism. According to pertinent statistics, the diameter of the current air suction seed metering drums ranges from 140 to 260 mm. Considering comprehensively, the drum diameter *D* was 205mm. The standard specification for tomato, hot pepper, and eggplant seedling trays were 72 holes (6 holes/row 12 rows), 530 mm in length, 270 mm in width, and 45 mm in height, respectively. The hole spacing was 40 mm. According to the specification requirements of the seedling tray, the number of axial holes of the seed metering drum was determined to be 6, and the hole spacing $L_k$ was 40mm, so the length $L_z$ of the left air chamber (shaped hole air chamber) was more than 200mm, which was taken as 220mm. The length of the right air chamber (the air chamber for the fan blade) was chosen at 130mm taking into account the passage and fan blade lengths. The total length of the drum was $L$=350mm. Considering the airflow disturbance generated by the fan blade, the air chamber was divided into two parts through the annular partition: the shaped hole air chamber and the fan blade air chamber. The geometric model of the drum is shown in Figure 5.

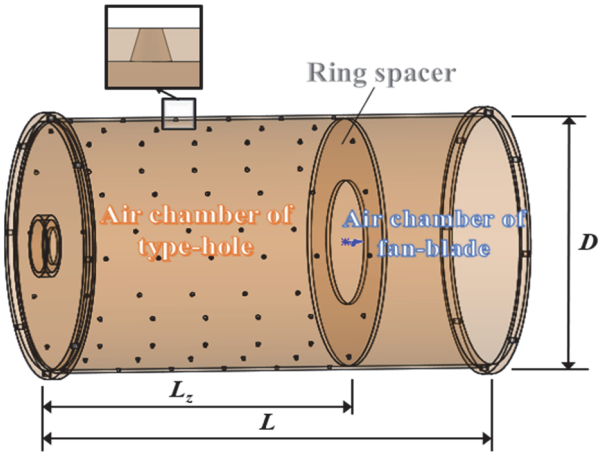


Figure 5. Geometric model of drum

**4. Simulation Experiment**

In the above, the hole entrance size and shape as well as the drum diameter and structure distribution were designed. The simulation verification and feasibility analysis of the hole and drum construction of the seed metering device were carried out with the appropriate CFD software since they are the important structures that influenced the seed suction efficiency of the device.

*4.1 Governing Equation and Turbulence Model*

To obtain the flow field pressure and velocity at the metering drum and the molded hole, the Navier-Stokes equation must be used to solve it, which describes the fluid motion under a given set of boundary conditions. These equations and turbulence models are solved at each node of the grid. Realizable k - ε Turbulence Model was used here. (lhan ztürk, 2019)

The continuity equation is as follows:

$$\frac{\partial \rho}{\partial t}+\frac{\partial}{\partial x_i}(\rho u_i)=0 \tag{5}$$

The equation for the conservation of momentum is as follows:

$$\frac{\partial}{\partial t}(\rho u_i)+\frac{\partial}{\partial x_i}\left(\rho u_i u_j\right)=-\frac{\partial p}{x_i}+\frac{\partial}{x_i}\left(\mu\frac{\partial u_i}{\partial x_i}-\rho\overline{u_i' u_j'}\right)+S_i \tag{6}$$

The turbulent kinetic energy and dissipation rate equations of the realizable k- ε turbulence model are as follows:

$$\frac{\partial(\rho k)}{\partial t}+\frac{\partial(\rho k u_i)}{\partial x_i}=\frac{\partial}{\partial xj}\left[\left(\mu+\frac{u_t}{\sigma_k}\right)\frac{\partial k}{\partial xj}\right]+G_k-\rho \tag{7}$$

$$\frac{\partial(\rho\varepsilon)}{\partial t}+\frac{\partial(\rho\varepsilon u_i)}{\partial x_i}=\frac{\partial}{\partial xj}\left[\left(\mu+\frac{u_t}{\sigma\varepsilon}\right)\frac{\partial\varepsilon}{\partial xj}\right]+\rho C_1 E_\varepsilon-\rho C_2\frac{\varepsilon^2}{k+\sqrt{v\varepsilon}} \tag{8}$$

where, $\mu_t$represents the eddy viscosity. σk and σε are the turbulent Prandtl numbers for k and ε, respectively. C1 = max[0.43, (η/η + 5)], where η = (2Eij•Eij) 1/2•k/ε., Eij=1/2($\partial\mu_i/\partial x_j+\partial\mu_j/\partial x_i$), C2 = 1.9.

*4.2 Mesh Generation*

The unstructured grid was used to mesh the simulation model, which has high adaptability and arbitrary structure. In this paper, the multiple reference frame (MRF) method was used, and the model was divided into two regions: dynamic region I and static region II.To ensure the accuracy of the subsequent solution calculation, a boundary layer was added to the fan blade wall and the cylinder boundary. According to the requirements of the wall function, $y^+$ was controlled between 30 and 300. (Di Zhu,2020)The mesh independence check was done to eliminate the influence of mesh size on the accuracy of the numerical simulation.As shown in Figure 6, where the error was less than 0.5% for 1.9 million or more grids. Based on the grid independence test, 2.0 million grids were generated in total, and the grid division is shown in Figure 7.

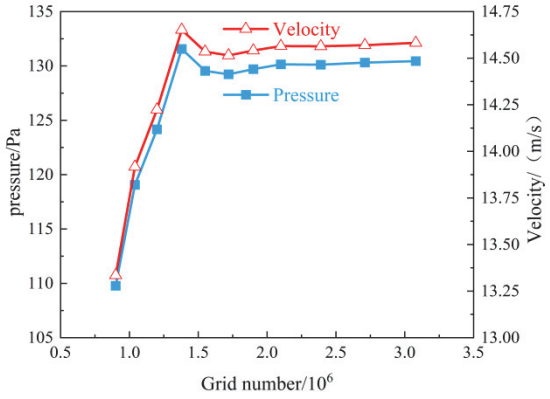


Figure 6. Grid Independence

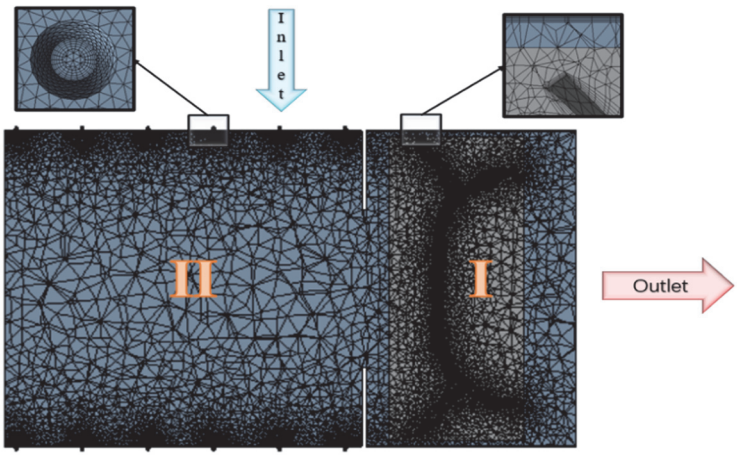


Figure. 7 Grid division

## 5. Simulation Results and Analysis

FLUENT was used to run numerical simulation tests. When the calculation residual is less than $1 \times 10^{-4}$, it is considered that the calculation results have converged. When the calculation result converged, the pressure and velocity nephogram of the molded hole inlet and the middle section were added as shown in Figures 8 and 9.

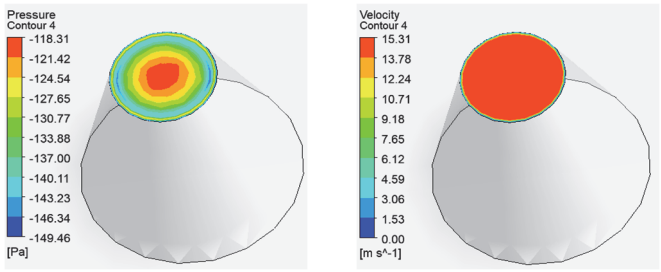


a b

Figure. 8 hole inlet: (a) Pressure nephogram (b) Velocity nephogram

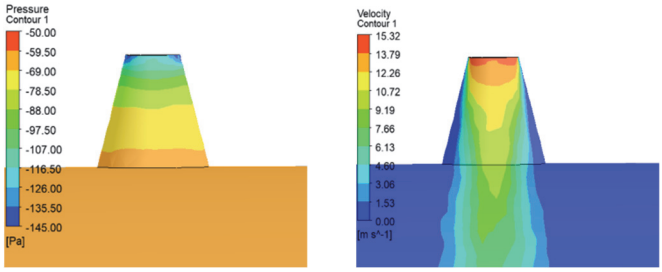


a b

Figure 9. Middle Section of hole: (a) Pressure Cloud Chart (b) Velocity Cloud Chart

As shown in Figure 8a, the edge color of the molded hole inlet surface was blue-green, while the middle color was orange-red, which meant that the negative pressure in the middle of the molded hole inlet was not equal to the edge, that is, the distribution of the negative pressure at the inlet was uneven, and it could be seen from the figure that the negative pressure at the inlet was between 118.31 and 149.46Pa, with a large fluctuation range. Therefore, it was necessary to use the surface area method to solve the surface weighted average value of the negative pressure at the inlet, and the result is 129.85Pa. According to the previous research, the negative pressure required for seed adsorption must be greater than 50Pa, so the negative pressure effect at the inlet of this type of hole met the requirements. Figure 8b showed that the velocity at the orifice inlet center is 15.31 m/s, and the color of the orifice inlet edge was the same as that of the middle (considering viscosity, the velocity at the most edge was ignored). This demonstrated that the velocity at the inlet was evenly distributed, which was helpful for seed adsorption. The

above findings demonstrated that the fluid flow was uniform and the pore structure might achieve negative pressure at the inlet, which initially satisfied the requirements of seed adsorption.

Figure 9a showed that the color of the air chamber from the mold hole inlet to the mold hole gradually changed from blue-green to orange-yellow, indicating that the negative pressure value gradually decreased, that is, the negative pressure value at the inlet was greater than that in the air chamber, so the mold hole had a good negative pressure effect. Figure 9b demonstrated how the color of the air chamber progressively changed from orange-red to turquoise from the orifice inlet to the orifice, showing that the velocity value gradually lowered and a higher air velocity was present at the orifice. The results above showed that the shaped hole's structural properties caused the inlet gas flow to be accelerated, which increased the negative pressure value without causing any loss and results in a superior adsorption effect.

In conclusion, the situation of negative pressure generated by this pore structure was consistent with the theoretical results derived from the flow continuity equation and Bernoulli equation above and has a good effect in generating a negative pressure, basically meeting the requirements of adsorption seeds.

As the axial spacing between the shaped holes was too large, the negative pressure in the holes might be uneven, which would lead to a significant reduction in the seed suction effect of the seed metering device. Therefore, it was necessary to study the uniformity of the negative pressure of the molded hole. There were 12 rows of molded holes on the seed metering drum, each row had 6 holes, a total of 72 holes, which were evenly distributed along the circumference of the seed metering drum. The surface integral method was used to calculate the weighted average of the negative pressure at the inlet of each type of hole. The results are shown in Figure 10.

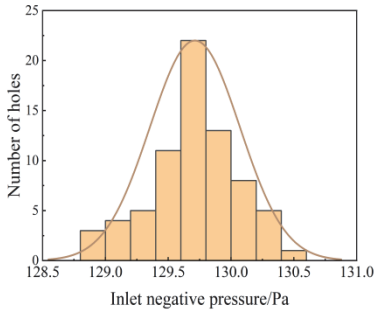


Figure 10. Distribution of Negative Pressure at the hole Inlet

Figure 10 showed that the negative pressure values at the entrance of 72 molded holes were concentrated between 128.75 and 130.75 Pa, which was an approximately normal distribution, indicating that this data was true and reliable, which preliminarily proved that the negative pressure at the entrance of molded holes was relatively uniform. A one-way ANOVA was carried out for the axial spacing of the orifice to investigate the uniformity of negative pressure at the orifice inlet further. Tables 2 and 4 display the outcomes of the data summary and analysis.

Table 2. Data summary

| Group | Observations | Sum | Average | variance |
|---|---|---|---|---|
| 1 | 12 | 1559.06 | 129.922 | 0.095 |
| 2 | 12 | 1555.84 | 129.653 | 0.139 |
| 3 | 12 | 1555.49 | 129.624 | 0.140 |
| 4 | 12 | 1555.87 | 129.656 | 0.035 |
| 5 | 12 | 1555.57 | 129.631 | 0.265 |
| 6 | 12 | 1557.46 | 129.788 | 0.076 |

Table 3 Analysis of variance

| Source of variance | SS | df | MS | F | P-value | F crit |
|---|---|---|---|---|---|---|
| Within group | 0.848 | 5 | 0.170 | 1.355 | 0.253 | 2.354 |
| Between groups | 8.264 | 66 | 0.125 | | | |
| Sum | 9.112 | 71 | | | | |

Table 2 showed that the average value range of the six groups of data was 129.624 to 129.922, and the variance range was 0.035 to 0.265. If the value fluctuation was small, the difference between the groups of data was not significant; Table 3 showed that $F=1.355<F_{crit}=2.354$, $P=0.253>0.05$, which meant that the difference between the data of each group was very small, that is, the axial spacing had no significant impact on the negative pressure at the entrance of the mold hole, so the negative pressure at the entrance between the holes of this structure was uniform.

As shown in Figure 11, added a vector and track map to the drum's inside and changed the scale factor and line size.

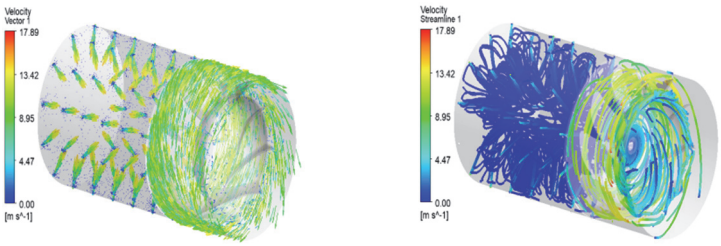


Figure 11. Vector and trace diagram inside the drum: (a) Vector diagram (b) Trace diagram

Figure 11a showed that the vector color at the orifice inlet gradually changed from blue to yellow-green, indicating that the velocity at the inlet tended to increase, which could be attributed to the acceleration of the incoming air flow due to the structural characteristics of the shaped hole. The color of the air chamber of the right fan blade was green, and the color was relatively uniform, indicating that the airflow velocity in the air chamber of the fan blade was relatively stable, which can be explained as that the airflow velocity is fast due to the rotation of the fan blade. Figure 11b showed that the trace color changed from light blue to dark blue from the molded hole inlet to the inside of the gas chamber, indicating that the flow rate of gas from the inlet to the gas chamber decreased gradually, which can be explained as the change of gas flow velocity caused by structural change when the gas entered the gas chamber from the molded hole. The trace colors of the left-side perforated air chamber and the right-side fan blade air chamber were different, which proved the effectiveness of the annular baffle to block airflow disturbance. The color of the middle trace of the air chamber of the right fan blade was different from the edge trace, which can be explained by the structural characteristics of the fan blade, resulting in the airflow speed at the edge of the cylinder being faster than that in the middle of the air chamber, and the gas was discharged along the edge of the cylinder. To sum up, according to the internal vector and track of the drum, the annular baffle blocked the airflow disturbance so that the airflow in the shaped hole air chamber was not affected, which was consistent with the original intention of the drum structure design above. However, the air velocity at the inlet of the shaped hole was higher than that in the air chamber of the shaped hole, which was consistent with the analysis conclusion at the shaped hole above.

As shown in Figure 12, added a pressure nephogram to the drum and adjusted the display range of the values was.

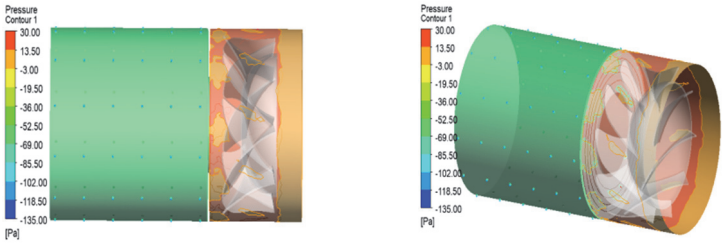


Figure 12. Cloud Chart of Drum Pressure Wall

Figure 12 showed that the wall pressure was divided into two parts: the pressure wall of the left orifice air chamber was green, indicating that the pressure here was negative and the value was very uniform. The wall color of the right fan blade air chamber was orange, indicating that the pressure here was positive and the value fluctuated slightly but was close. This result once again proved the effectiveness of annular baffles in preventing airflow disturbances. Since the airflow in the shaped hole air chamber was not disturbed by the airflow in the fan blade air

chamber, the internal negative pressure was uniform, providing a good air chamber environment for the seed metering device to adsorb seeds.

Created the XY section of the drum and added the pressure and speed nephogram, as shown in Figure 13.

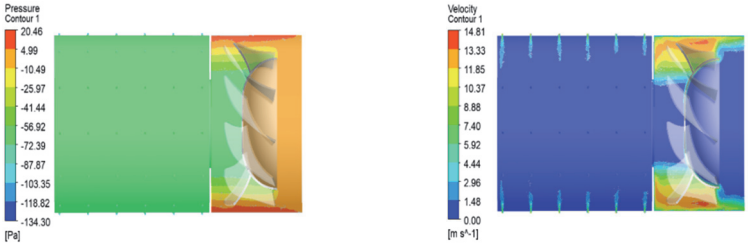


a b

Figure 13. Cloud Chart of XY Section: (a) Pressure Cloud Chart (b) Velocity Cloud Chart

Figure 13a showed that the pressure in the XY segment ranged from -134.30 to 20.46 Pa. The edge of the fan blade air chamber and the air outlet were under positive pressure, while the left-shaped hole air chamber and the middle of the right fan blade air chamber were under uniform negative pressure. This may be explained by the fact that the annular partition blocked the air flow disturbance generated by the rotation of the fan blade, which caused the negative pressure in the shaped hole air chamber not to be disturbed. In Figure 13b, it is depicted that the XY section's velocity ranged from 0 to 14.81 m/s.The velocity at the left-shaped hole air chamber was higher than that at the center of the air chamber, which was consistent with the results of the previous analysis on the shaped hole.

In conclusion, the annular baffle had a good effect in blocking the airflow disturbance, and due to the structural characteristics of the molded hole, the incoming airflow was accelerated, which further improved the negative pressure effect at the entrance and further improved the theoretical effect of seed adsorption. Therefore, the structure of the seed metering device designed in this study was reasonable, with high theoretical feasibility and reliability.

## 6. Bench Experiment

The seed metering performance was evaluated to confirm the viability and dependability of the real functioning of the axial air suction drum seed metering mechanism. Tomato, pod pepper, and eggplant seeds were employed in this study as sowing items. Relevant components of the seed measuring system were processed with 3D printing technology using white ABS resin as the material. The test bench was constructed of aluminum alloy profiles, as shown in Figure 14. Fan blades and seed metering drum were driven by a PUSS speed regulating motor and induction speed motor (4IK25GN-C) respectively.

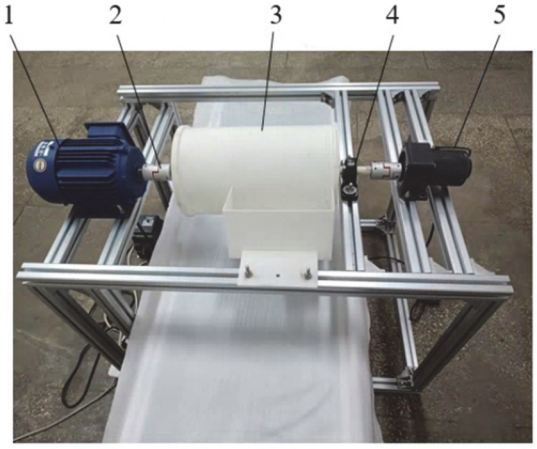


Figure 14. Test bench of axial air suction drum seed metering device: 1. PUSS speed regulating motor 2. Coupling 3. Seed metering device 4. Seat bearing 5. Induction speed motor

The seed metering drum designed in this paper had 72 holes. Combined with the structure size of the drum and the productivity of 600 plates/h of the seeder, the drum speed could be calculated as 8.6 r/min. The speed of the seed-

metering device was taken as a fixed parameter, and the speed of the fan blade was taken as a variable working parameter. The test results are shown in Table 4.

Table 4. Relationship between fan speed and seed adsorption rate

| Speed/rpm | Seed adsorption rate of tomato /% | Seed adsorption rate of pod pepper /% | Seed adsorption rate of eggplant/% |
|---|---|---|---|
| 1500 | 65.56 | 67.50 | 76.67 |
| 1800 | 76.39 | 76.67 | 85.28 |
| 2100 | 86.39 | 87.22 | 93.06 |
| 2400 | 95.56 | 96.11 | 98.06 |

As can be seen from the above table, the adsorption rate of the seed metering device on tomato seeds, jalapeno seeds, and eggplant seeds reached 86.39,87.22, and 93.06%, respectively, when the rotating speed reached 2100 rpm. When the rotating speed was 2400 rpm, the adsorption rate of the planter on tomato, hot pepper, and eggplant seeds reached more than 95%, which was higher than 90.83% of the qualified rate of sowing of other seed metering devices such as Li's pneumatic cylinder precision seeder (Li M, 2013) and 86% of the accuracy rate of sowing of small grain vegetable electric seeder developed by Du. (Du Z,2017) Therefore, the seed metering device designed in this paper had good seed suction performance.

## 7. Conclusions

In this paper, based on the principle of axial flow fan, flow continuity equation, and Bernoulli equation, an axial suction drum type seed metering device was designed. Its geometric model was established using 3D modeling software. The model pre-processing, mesh generation, and numerical simulation was carried out using CFD-related software, which verified the feasibility of the theoretical operation of the seed metering device. The feasibility and reliability of the actual operation of the seed metering device were verified by bench tests. The following conclusions are drawn based on the aforementioned analyses:

1) The mesh independence check was done to eliminate the influence of mesh size on the accuracy of the numerical simulation. The results showed that: For 1.9 million or more grids, the error was less than 0.5% Thus, based on the grid independence test，2.0 million grids were generated in total.
2) The numerical simulation results showed that the airflow at the inlet was accelerated due to the structural characteristics of the shaped hole, and the negative pressure effect at the inlet was therefore improved. According to the surface integration method, the average negative pressure at the orifice inlet was 129.85Pa. According to the previous research, the negative pressure required for seed adsorption was>50Pa, so it met the design requirements. The single factor variance analysis of the axial spacing of the molded holes showed that the axial spacing had no significant effect on the negative pressure at the entrance of the molded holes, so the uniformity of the negative pressure at the entrance between the various molded holes of the structure was good. The annular baffle in the drum effectively blocked the airflow disturbance, making the negative pressure effect in the shaped hole air chamber not affected by the fan blade air chamber.
3) The bench test results showed that when the fan blade speed reached 2100 rpm, the adsorption rates of the seed metering device on tomato pepper and Chaotian seed were more than 85%, and the adsorption rate on eggplant seed was more than 93.06%. When the fan blade speed reached 2400 rpm, the seed metering device could adsorb more than 95% of tomato, hot pepper, and eggplant seeds, indicating that the seed metering device had good seed adsorption performance.
4) The air-suction drum seed-metering device might be constructed much more simply since it did not require a particular vacuum pump and associated pipeline facilities, which greatly simplified the structure of the air-suction drum seed-metering device, and provided a reference for optimizing and improving the key components of the facility seedling precision seeder.

**Acknowledgments**

This study was funded by Major science and technology projects in Yunnan Province (grant number 202102AE090042-06) and Major science and technology projects in Yunnan Province (grant number 2018ZC001-4)

The authors declare that they have no conflict of interest.

**Compliance with Ethical Standards**

**Funding** This study was funded by Major science and technology projects in Yunnan Province (grant number 202102AE090042-06) and Major science and technology projects in Yunnan Province (grant number 2018ZC001-4)

**Conflicts of interest** The authors declare that they have no conflict of interest.

**References**

Chen, H. T., Wang, H. F., & Wang, Y. C. (2020). Design and Experiment of Three-leaf Type Air-suction Seed Meter with Automatic Clear and Replace Seeds Features for Soybean Plot Test. *Transactions of the Chinese Society of Agricultural Machinery, 51,* 75-85. https:// doi.org/ 10.6041/j.issn.1000-1298.2020.12.008

Di Zhu, Ruofu Xiao, & Zhifeng, Y. (2020). Optimization design for reducing the axial force of a vaned mixed-flow pump. *Engineering Applications of Computational Fluid Mechanics, 14,* 882-896. https:// doi.org/10.1080/19942060.2020.1749933

Ding, L, Yang, L, & Liu, S, R. (2018). Design of air suction high speed precision maize seed metering device withb assistant seed filling plate. *Transactions of the Chinese Society of Agricultural Engineering, 34,* 1-11. https://doi.org/10.11975/j.issn.1002-6819.2018.22.001

Du, Z, Shu, H. J, & Lu, Z. M., et al. (2017). Design and manufacture of seed planter for small grain vegetable. *Journal of Chinese Agricultural Mechanization, 38,* 5-10.

Ji, Y., Zhang, W. Y., & Liu, H. J. (2021). Design and experiment of double-layer drum precision seed sowing device. *Journal of Chinese Agricultural Mechanization, 42,* 22-28.

Jiang, Y. Z., Hou, X. X., & Zhao, Y. M. (2019). Design and experiment of air suction drum precision metering device for air blowing and seeding. *Journal of Gansu Agricultural University, 54,* 211-218.

Karayel, D. (2009). Performance of a modified precision vacuum seeder for no-till sowing of maize and soybean. *Soil and Tillage Research, 104*, 121-125. https:// doi.org/10.1016/j.still.2009.02.001

lhan, ztürk, Cenk, E., & Mehmet, M. Y. (2019). Effect of fan and shroud configurations on underhood flow characteristics of an agricultural tractor. *Engineering Applications of Computational Fluid Mechanics, 13,* 506-518. https:// doi.org/10.1080/19942060.2019.1617192

Li, M., Liu, X. H., & Liao, Y. T., et al. (2013). Pneumatic Cylinder-type Centralized Precision Metering Device for Rapeseed. *Transactions of the Chinese Society of Agricultural Machinery, 44,* 68-73. https:// doi.org/10.6041/j.issn.1000-1298.2013.12.012

Li, Z. G., Yang, Q. C., & Sha, D. J. (2022). Research progress on the full mechanization production of hydroponic leafy vegetables in plant factory. *Journal of China Agricultural University, 27,* 12-21.

Liu, Y., Yang, S. D., & Wei, Z. C. (2022). Reviews on technology and equipment of sugarbeet production. *Journal of Chinese Agricultural Mechanization, 43,* 36-46.

Sun, H, Guo, G. C., & Tang, S. (2021). Improvement of hole pressing drum device and design of the control system for vegetable seedling's seeding assembly line. *Transactions of the Chinese Society of Agricultural Engineering, 37,* 41-48.

Wang, L. H., Fang, Z. Y., & Du, Y. C. (2016). Study on Development Strategy of Vegetable Seed Industry in China. *Strategic Study of CAE, 18*, 123-136.

Wang, X. Y., Liao, Q. X., & Liao, Y. T. et al. (2021). Situation and prospect of key technology and equipment in mechanization and intelligentization of rapeseed whole industry chain. *Journal of Huazhong Agricultural University, 40,* 24-44.

Xu, S. Y., Li, Y., & Qi, X. D. (2020). Design of Pneumatic Precision Seed Metering Device for Carrot. *Journal of Agricultural Mechanization Research, 42,* 46-51.

Yang, C. M., Yi, W. Y., & Qiu, Y. Q. (2022). Research status and development analysis of seed-raising precision seeder. *Journal of Chinese Agricultural Mechanization, 43,* 183-188.

Yang, C. M., Zhuang, W. H., & Xu, Y. (2020). Study on vegetable tray precision seeder. *Journal of Chinese Agricultural Mechanization, 41,* 13-18.

Yin, W. Q., Zhao, Lu., & Li, H. (2019). Design and Experiment on Suction Nozzle Type Hole of Pneumatic-sheave

Combined Vegetable Precision Metering Device. *Transactions of the Chinese Society of Agricultural Machinery, 50*, 68-76. https:// doi.org/10.6041/j.issn.1000-1298.2019.04.008

Zhang, H., Luo, X., & Jiang, Y. Z. (2019). Experimental Study on the Performance of Double Cavity Metering Roller for Tomato Seedling Planter. *Journal of Agricultural Mechanization Research, 41,* 164-170.

Zhang, X. H., Wong Y. Z., & Zhang, L. (2018). Design and Experiment of Wheat Pneumatic Centralized Seeding Distributing Syste. *Transactions of the Chinese Society of Agricultural Machinery, 49,* 59-67. https:// doi.org/10.6041/j.issn.1000-1298.2018.03.007

Zhang, X. L., Song, J., & Li, X. Y. (2020). Design and simulation analysis of pneumatic mechanical combined single disc and double row seed meter. *Journal of Chinese Agricultural Mechanization, 41,* 30-34.

Zhao R. (2022). Study on Mechanized Precision Sowing Technology of Protected Vegetable Seedling. *Agricultural Technology & Equipment, 43,* 43-48.

Zhu, L. T, Liao, Q. X., & Liu, H. (2022). Design and test of the seeding amount control system for the rape mechanical metering device. *Transactions of the Chinese Society of Agricultural Engineering, 38,* 19-29. https://doi.org/10.11975/j.issn.1002-6819.2022.10.003